ACS APPLIED MATERIALS & INTERFACES

Research Article

Cite This: ACS Appl. Mater. Interfaces 2020, 12, 2591−2600

www.acsami.org

Cobalt/Nickel Ions-Assisted Synthesis of Laminated CuO Nanospheres Based on $Cu(OH)_2$ Nanorod Arrays for High-Performance Supercapacitors

Aitang Zhang,[†] Lijun Yue,[†] Dedong Jia,[†] Liang Cui,[*,‡] Di Wei,[‡] Weiguo Huang,[†] Rui Liu,[†] Ying Liu,[†] Wenrong Yang,[§] and Jingquan Liu[*,†,‡]

[†]College of Materials Science and Engineering, Institute for Graphene Applied Technology Innovation, Collaborative Innovation Centre for Marine Biomass Fibers, Materials and Textiles of Shandong Province, Qingdao University, Qingdao 266071, Shandong, China

[‡]College of Materials Science and Engineering, Linyi University, Linyi 276000, Shandong, China

[§]Centre for Chemistry and Biotechnology, School of Life and Environmental Sciences, Deakin University, Geelong Waurn Ponds Campus, Geelong, VIC 3216, Australia

Supporting Information

ABSTRACT: The development for environmentally friendly energy conversion and storage equipment has given rise to tremendous research efforts as a result of the growing requirements for environmental friendly resources and the rapid consumption of traditional fossil fuel. Herein, a novel hierarchical CoO/NiO−Cu@CuO heterostructure is successfully devised and synthesized. Cobalt/nickel ions are used to generate novel CoO/NiO-doped laminated CuO nanospheres through the facile in situ wet oxidation combined with cation exchange and calcination strategies. As a result, the electrochemical supercapacitance of the as-prepared CoO/NiO−Cu@CuO electrode can reach 875 C cm^{-2} (2035 mF cm^{-2}), which exhibits much better electrochemical performance compared to other precursor electrodes at a same current density of 2 mA cm^{-2}. Moreover, an excellent rate capacity of 1395 mF cm^{-2} (50 mA cm^{-2}) can be achieved when measured at a relative high current density; 90.3% of the initial supercapacitance remains even after 5000 cycles. Furthermore, the as-prepared hierarchical hybrid of laminated CoO/NiO−CuO nanospheres in situ generated on three-dimensional (3D) porous Cu foam is applied to prepare a solid-state asymmetric supercapacitor equipment unit. The fabricated equipment unit shows an energy density of 69.3 W h kg^{-1} at a power density of 1080 W kg^{-1}. Additionally, the commercially applied 2.5 V light-emitting-diode indicator with blue light can be energized for 4 min when two as-fabricated supercapacitor devices are in series connection. The unique hierarchical heterostructure of the novel laminated nanospheres combined with the 3D grid structure brings about the outstanding electrochemical capacitor performances. This strategy for the fabrication of hierarchical heterostructure electrodes could have an enormous potential for high-performance electrochemical equipment.

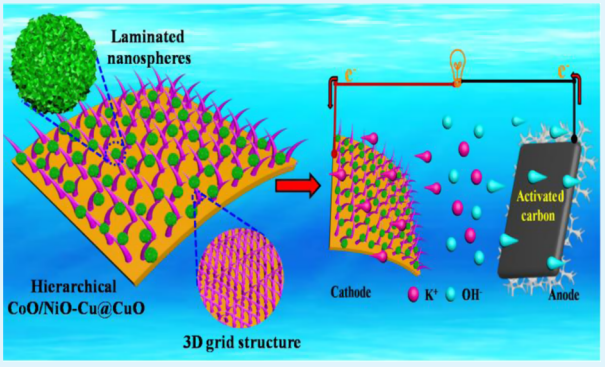

KEYWORDS: *laminated nanospheres, hierarchical heterostructure, in situ generated, CoO/NiO−Cu@CuO, supercapacitors*

1. INTRODUCTION

Tremendous research attention has been dedicated to explore environmentally friendly energy-conversion and -storage nanomaterials owing to the growing requirements for sustainable energy sources and the vast consumption of traditional fossil fuels.[1,2] In particular, developing high-efficiency energy storage devices is an urgent need for driving various kinds of electric automobile, electronic equipment, and handy facility.[3−6] As an important component of the sustainable energy devices, electrochemical energy storage equipment has attracted extensive attention and has become an important candidate for energy storage gradually.[7] After a period of time, electrochemical supercapacitors (SCs) have become one of the most important alternates owing to their ultrahigh power and energy densities, admirable safety, and super-recyclability compared to the traditional storage equipment, such as the rechargeable batteries.[4,8−10] Graphene, carbon nanotubes, and other carbon materials with large specific surface area, extraordinary chemical stabilization, and excellent conductivity characteristics in general store energy through the electrostatic adsorption and desorption mechanism at electrode and electrolyte interfaces, which are commonly regarded as

Received: November 18, 2019
Accepted: December 23, 2019
Published: December 23, 2019

DOI: 10.1021/acsami.9b20995
ACS Appl. Mater. Interfaces 2020, 12, 2591−2600

electrical double-layer capacitor-type electrode materials.[10] While pseudocapacitors store energy mainly through the fast and reversible faraday redox reactions on the basis of transition-metal oxides/hydroxides/sulfides and conductive polymers.[2,11] Furthermore, the specific capacitance and energy density of pseudocapacitor are usually higher than those of EDLC because of the fast faraday redox reactions.[3,6,12] For achieving high-performance SCs, the electrode materials are needed to have a large specific area, high conductivity, low fabrication cost, abundant active sites, and satisfactory electrochemical stability.[13] Many kinds of material system have been designed and prepared to improve the electrode performances, among which the redox-active transition-metal oxides with desirable conductivity and high reactive oxidation states exhibit huge advantages in the supercapacitor fields.[5,7,14]

Ruthenium dioxide was extensively utilized as an excellent electrode material for electrochemical storage devices among various transition-metal oxides. However, the drawbacks of high cost and toxicity severely limit the practical applications. Hence, it is necessary to exploit new, low-cost electrode materials.[15,16] Recently, copper oxide (CuO) has attracted significant attention on account of its low cost, eco-friendliness, extensive sources, and ultrahigh specific capacitance.[17−21] For its application in pseudocapacitors, the theoretical pseudocapacitance of CuO was approximately 1800 F g^{-1}.[3,22] In consequence, various strategies have been explored for the preparation of diverse nanostructures for copper oxide.[23,24] Nevertheless, the single-phase metal oxide was limited by the poor ion-diffusion rate and electrochemical stability, which may be unable to meet the growing high requirements.[4,7,25] To solve the above problems, one strategy is to develop hybrid nanocomposites with various hierarchical structures and unique morphologies, especially in the form of hierarchical nanoarrays directly generated on substrates to enhance the electrochemical conductivity.[26] Such hierarchical nanoarrays could be directly employed as electrodes for electrochemical applications.[4,7,10,23] Furthermore, efforts aiming to enhance the supercapacitor properties based on copper chalcogenide still face challenges, and achieving high capacitance for practical application is still in urgent demand.[3,27]

In this work, novel laminated CoO/NiO−CuO nanospheres were generated with the assistance of cobalt/nickel ions via a facile in situ wet oxidation combined with cation exchange and calcination strategies. In addition, the as-prepared hierarchical heterostructure of CoO/NiO−Cu@CuO was directly utilized to prepare a freestanding electrode, which displayed an outstanding electrochemical supercapacitor performance. The fabricated CoO/NiO−Cu@CuO electrode presented an outstanding supercapacitance of 875 C cm^{-2} (2035 mF cm^{-2}) at 2 mA cm^{-2}. Moreover, an excellent rate capacity of 1395 mF cm^{-2} (50 mA cm^{-2}) can be achieved when measured at a relatively high current density; 90.3% of the initial supercapacitance remains even after 5000 cycles. The as-prepared asymmetric supercapacitor (ASC) equipment unit exhibited an energy density of 69.3 W h kg^{-1} at a power density of 1080 W kg^{-1}. Furthermore, the commercially applied 2.5 V light-emitting-diode indicator with blue light can be energized for 4 min when two as-fabricated supercapacitor equipment units are in series connection. Therefore, the prepared hierarchical heterostructure of CoO/NiO−Cu@CuO could have an enormous potential for the preparation of ultrahigh-performance electrochemical equipment for practical applications.

2. EXPERIMENTAL SECTION

2.1. Reagents. All of the nickel and copper foams were bought from Shanghai Zhongwei New Material Co., Ltd. Hydrochloric acid was produced by Tianjin Fuyu Fine Chemical Co., Ltd. Acetone, ethanol, sodium hydroxide (NaOH, AR), potassium hydroxide (KOH, AR), acetylene black (AR), activated carbon (AC), sodium thiosulfate pentahydrate ($Na_2S_2O_3·5H_2O$, AR), ammonium persulfate ($(NH_4)_2S_2O_8$, AR), polyvinylidene fluoride (PVDF, AR), cobalt(II) chloride hexahydrate ($CoCl_2·6H_2O$, AR), and nickel(II) chloride hexahydrate ($NiCl_2·6H_2O$, AR) were all bought from Sinopharm Chemical Reagent Co., Ltd. The above-mentioned chemicals were utilized as bought without any purifications. The used deionized water was produced by a Flom ultrapure water instrument with a resistivity of 18.2 MΩ cm^{-1}.

2.2. Synthetic Strategy of $Cu(OH)_2$ Nanorods. Typically, the bought Cu foam was ultrasonically washed with hydrochloric acid, acetone, ethanol, and deionized water and placed in a vacuum oven under 50 °C to be dried adequately. Typically, 2.5 mol NaOH aqueous solution (10.0 mL) and 0.125 mol $(NH_4)_2S_2O_8$ aqueous solution (10.0 mL) were mixed. Then, a uniform transparent solution would be achieved by continuous stirring. Subsequently, the dealt Cu foam was then placed into a preprepared solution for 10 min at the ambient temperature. After the reaction, the resulting light blue Cu foam was cleaned using deionized water. Later, $Cu@Cu(OH_2)$ was obtained through drying at 50 °C in the vacuum oven. Additionally, the mass loading of $Cu(OH_2)$ nanorods is 3.1 mg cm^{-2}.

2.3. Synthesis of CuO Nanowires. Cu@CuO was generated via a calcination procedure from the prepared $Cu@Cu(OH_2)$ precursor. In a typical procedure, $Cu@Cu(OH_2)$ underwent thermal treatment through a tubular furnace and exposed to a nitrogen atmosphere with a flow of 5 °C min^{-1} at 200 °C for 2 h. Subsequently, brownish black Cu@CuO nanoarrays were obtained. The mass load of CuO nanowires is approximately 2.5 mg cm^{-2}.

2.4. Preparation of CoO/NiO-Doped Laminated CuO Nanospheres on Copper Foam (CoO/NiO−Cu@CuO). The CoO/NiO-doped novel laminated CuO nanospheres were generated with the assistance of Co^{2+} and Ni^{2+} ions using CuO nanowires as precursor. Briefly, 12 mg of $CoCl_2·6H_2O$ and 12 mg of $NiCl_2·6H_2O$ were dispersed into 70 mL of a mixed solvent containing 30 mL of ethanol and 40 mL of deionized water to achieve a homogeneous solution. In addition, a comparison sample was also prepared without adding $CoCl_2·6H_2O$ and $NiCl_2·6H_2O$. Subsequently, 40 mL of 1.5 M $Na_2S_2O_3·5H_2O$ was added to the preprepared solution dropwise and stirring for 30 min. The generated Cu@CuO nanowires were immersed in the above-mentioned suspension at an ambient temperature for 3 h. After that, the obtained product was cleaned with deionized water repeatedly and subsequently dried in an oven. Finally, the generated CoO/NiO-doped laminated Cu@CuO nanospheres on three-dimensional (3D) copper foam was calcined in a tube furnace and exposed to an air atmosphere at 300 °C for 2 h. After that, a black copper foam was obtained. The mass of CoO/NiO−CuO nanospheres is found to be about 2.3 mg cm^{-2}.

2.5. Instruments. The structure and morphology of the synthesized materials were analyzed by a scanning electron microscope working at a voltage of 10 kV, and the relevant energy-dispersive X-ray spectroscopy (EDX) elemental mapping images were taken through a scanning electron microscope of JEOL JSM-6700F with a potential of 20 kV. X-ray photoelectron spectroscopy (XPS) measurements were carried out through a spectrometer of Kratos Axis Ultra DLD. The crystalline compositions of the synthesized samples were measured by an X-ray diffractometer with Cu Kα radiation.

2.6. Electrochemical Performance Tests. The supercapacitor performances were measured in a 6 M KOH aqueous solution through the electrochemical workstation. In the three-electrode measurement, the fabricated material (1.0 × 1.0 cm^2) was applied as the working electrode, while the Pt as negative and HgO as the reference electrodes. At different scan rates, the cyclic voltammetry (CV) curves were measured in the voltage range of 0.15−0.58 V. Meanwhile, the galvanostatic charge/discharge (GCD) curves were

DOI: 10.1021/acsami.9b20995
ACS Appl. Mater. Interfaces 2020, 12, 2591−2600

Scheme 1. Schematic Diagram for the Stepwise Synthesis of Novel Laminated CoO/NiO−CuO Nanospheres in Situ Generated on CuO Nanowire Arrays Precursor with the Assistance of Cobalt/Nickel Ions

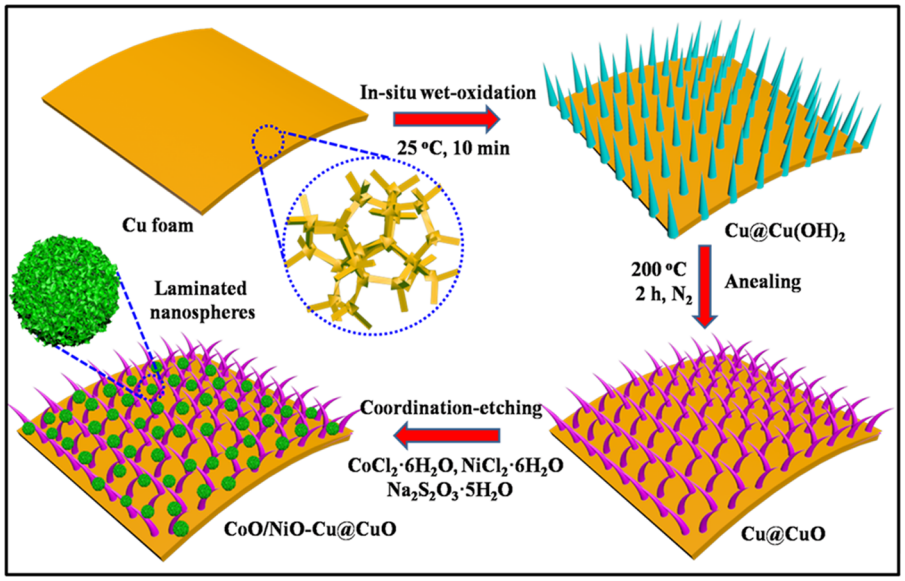

also measured under the same range at different current densities. Electrical impedance spectroscopy (EIS) was tested at an open-circuit potential of 5 mV, and AC disturbance ranges from 0.01 Hz to 100 kHz frequency response. The electrochemical specific capacitances were figured out through the below equation

$$C_A = \frac{I\int V\Delta t}{sV^2} \tag{1}$$

where C_A (F cm^{-2}) is the areal supercapacitance, I_A represents the current of discharge, t (s) refers to the time of discharge, V (V) means the voltage range, and s (cm^2) is the reacted acreage of the material.

2.7. Preparation of KOH/PVA Hydrogel Electrolyte. Typically, 2 g of PVA was immersed in 20 mL of deionized water at the temperature of 80 °C with continuous vigorous stirring to get a homogeneous solution. As a result, a clear viscous solution was obtained after 3 h. After the solution was cooled to about 65 °C, 10 mL of 6 M KOH aqueous solution was then dropped into the preprepared solution and stirred constantly until complete dissolution and formation of a jell-like solution, which was then cooled to ambient temperature to obtain the KOH/PVA hydrogel electrolyte for further use.

2.8. Preparation of an All-Solid-State Asymmetric Supercapacitor (ASC) Equipment Unit and the Electrochemical Tests. Polyvinylidene fluoride (PVDF), acetylene black, and active carbon were dispersed into ethanol in a ratio of 8:1:1 to achieve a homogeneous solution. The target material was obtained after drying in vacuum at 50 °C for 5 h. Subsequently, 10 mg of prepared products were embedded into the nickel foam with the area of 1.0 × 1.0 cm^2. Then, the ASC device was prepared by applying the as-prepared CoO/NiO−Cu@CuO (1.0 × 1.0 cm^2) as the working electrode and AC as the counter electrode, as well as the preprepared KOH/PVA hydrogel served as the solid gel electrolyte. Typically, the as-prepared freestanding CoO/NiO−Cu@CuO and AC-coated nickel foam electrodes were attached on copper films, which worked as a current collector. Subsequently, the preprepared solid gel electrolyte was applied on the external surface of the CoO/NiO−Cu@CuO and AC-coated nickel foam electrodes until saturation. Then, the CoO/NiO−Cu@CuO and AC-coated nickel foam electrodes were pressed together with little pressure to enable the KOH/PVA gel electrolyte on each electrode to combine into one thin separating layer to achieve the CoO/NiO−Cu@CuO//AC ASC device. Compared to the supercapacitors packed with aqueous electrolytes and a separator, the polymer gel electrolytes of KOH/PVA exhibit excellent safety and stability. Additionally, the charges of the working and counter electrodes should maintain a equilibrium relationship, which is calculated based on the below equation[28]

$$q = C \times m \times \Delta V \tag{2}$$

where C (F g^{-1}) refers to the mass capacity, m (g) represents the active product mass, V (V) refers to the voltage range, and q represents the charge loaded in electrode. In addition, the mass ratio (m^+/m^-) of electroactive material between two electrodes can be obtained through the below equation

$$m^+/m^- = C^-\Delta V^-/C^+\Delta V^+ \tag{3}$$

where the electrochemical supercapacitance (F g^{-1}) of the synthesized electrode materials can be evaluated by utilizing C^+ and C^-. V^+ (V) and V^- (V) represent the potential range of the synthesized sample and active carbon electrodes, respectively. In addition, the electrochemical supercapacitance (C_s) of the ASC can be gained through the below equation

$$C_s = \frac{I\int V\Delta t}{mV^2} \tag{4}$$

where I (A) refers to the current of discharge, t (s) represents the time of discharge, V (V) means to the voltage window, and m (g) refers to the active product mass. Moreover, the energy density E (W h kg^{-1}) and power density P (W kg^{-1}) can be obtained through the equation as illustrated below

$$E = \frac{1}{2}C_s\Delta V^2 \tag{5}$$

$$P = E/\Delta t \tag{6}$$

3. RESULTS AND DISCUSSION

The stepwise fabrication of novel hierarchical CoO/NiO−CuO nanospheres generated with the assistance of cobalt/nickel ions based on CuO nanowire arrays precursor is schematically illustrated in Scheme 1. After the in situ wet oxidation procedure, the 3D substrate of Cu foam was all overgrown with $Cu(OH)_2$ nanorods. Subsequently, bunchlike Cu@CuO nanowires with slightly curly and connected tops were derived through the calcination treatment of its Cu@$Cu(OH)_2$ nanorods precursor. The CoO/NiO-doped CuO

DOI: 10.1021/acsami.9b20995
ACS Appl. Mater. Interfaces 2020, 12, 2591−2600

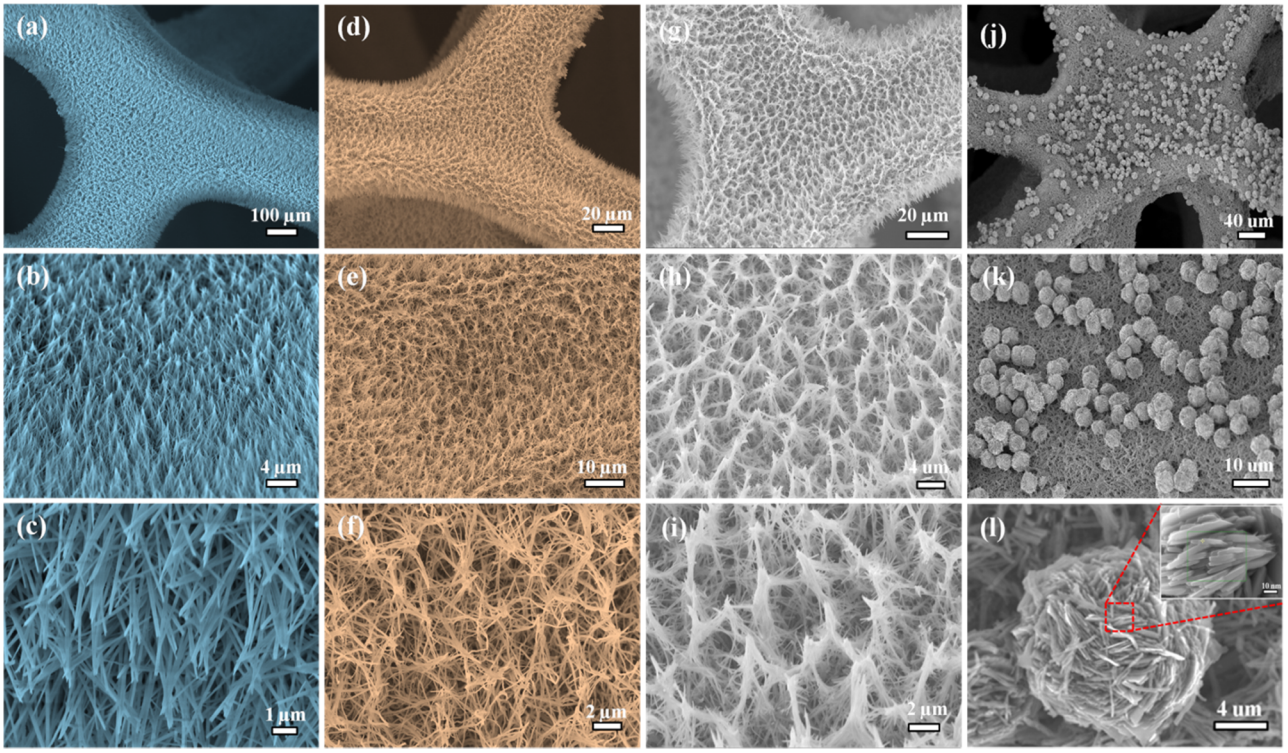

Figure 1. SEM images of (a–c) Cu@Cu(OH)$_2$ nanorod arrays, (d–f) Cu@CuO nanowire arrays, (g–i) the comparison sample without adding Co^{2+} and Ni^{2+} ions, and (j–l) CoO/NiO-doped laminated CuO nanospheres.

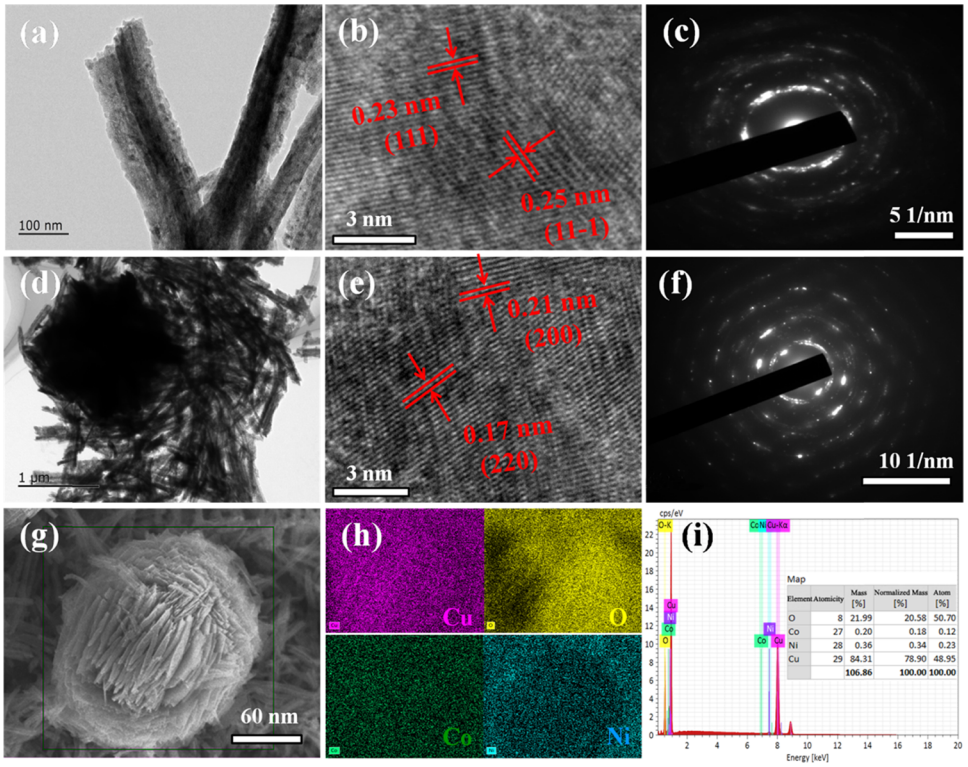

Figure 2. (a) TEM, (b) HRTEM, and (c) the corresponding SAED images of Cu@CuO. (d) TEM, (e) HRTEM, and (c) the corresponding SAED images of CoO/NiO–Cu@CuO. (g) SEM image and the (h) EDX elemental mapping images of CoO/NiO–Cu@CuO. (i) EDX spectrum of CoO/NiO–Cu@CuO.

nanospheres were generated with the assistance of Co^{2+} and Ni^{2+} ions, followed by calcination treatment. Interestingly, the obtained CoO/NiO-doped laminated CuO nanospheres were generated from the rearranged CuO nanowires, which are tightly bound together. Cobalt/nickel ions were doped into the laminated CuO nanospheres during the cation exchange

DOI: 10.1021/acsami.9b20995
ACS Appl. Mater. Interfaces 2020, 12, 2591–2600

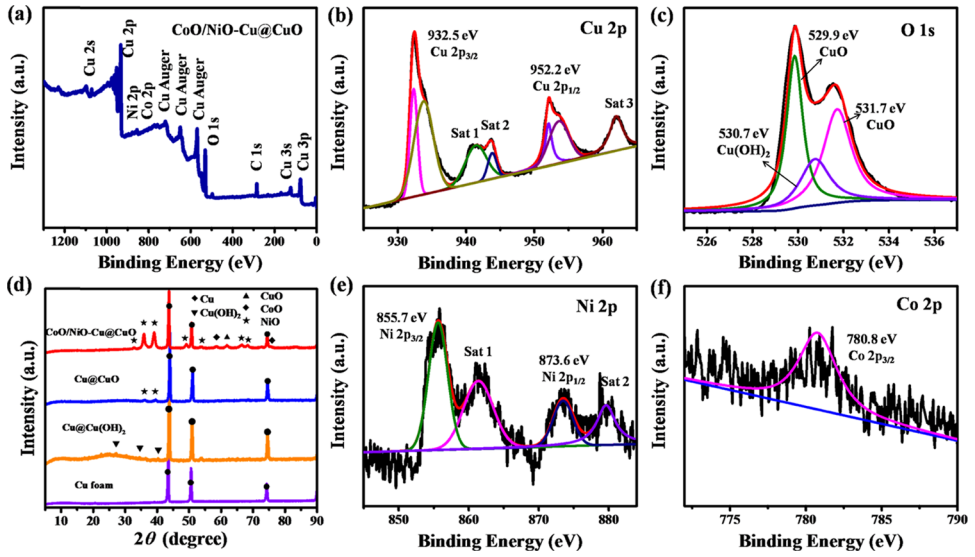

Figure 3. (a) Survey XPS spectrum and high-resolution spectra for (b) Cu 2p, (c) O 1s, (e) Ni 2p, and (f) Co 2p of the as-prepared hierarchical heterostructure of CoO/NiO−Cu@CuO. (d) XRD patterns of all synthesized samples.

process. After calcination process, the CoO/NiO-doped CuO nanospheres were obtained. This unique and novel characteristic hierarchical heterostructure with 3D grid structure and laminated nanospheres possesses a large specific surface area and accelerates the charge transfer rate as well as the redox reactions during electrochemical applications.

The structures of the stepwise synthesized samples were first characterized by scanning electron microscopy (SEM). Cu@CuO nanowires were generated through a facile calcination process of its Cu@$Cu(OH)_2$ nanorods precursor. The SEM image (Figure S2) of the bare Cu foam shows that Cu foam has a 3D porous structure with micrometer-sized pores, demonstrating that Cu foam can be utilized as a good template for surface modification. As clearly observed from Figure 1a−c, the utilized Cu foam was completely overgrown with intersected $Cu(OH)_2$ nanorods after in situ oxidation treatment, and the Cu foam still remained the 3D grid structure. $Cu(OH)_2$ was gradually transformed into CuO during the calcination treatment; meanwhile, the bunchlike nanowire arrays were formed as shown in Figure 1d−f. The diameter of the obtained CuO nanowire is approximately 105 nm, which is thinner than the $Cu(OH)_2$ nanorod of 158 nm. Interestingly, the Cu foam with reddish brown color was turned into brilliant blue after wet oxidation and then changed to brownish black after calcination treatment at 200 °C, as shown in Figure S1, indicating the phase transformations. The CoO/NiO-doped CuO nanospheres are generated with the assistance of Co^{2+} and Ni^{2+} ions through the cation exchange strategy and calcination treatment. The obtained products exhibit a totally different appearance, as shown in Figure 1j−l. Low-magnification SEM images show that the generated CoO/NiO-doped CuO nanospheres are homogeneously distributed on the newly generated 3D grid structure that are fully covered with slightly curly and tops tangled CuO nanowires. Moreover, the resulting CoO/NiO-doped laminated CuO nanospheres are generated from the rearranged CuO nanowires, which are tightly bound together, as clearly shown in Figures S3 and 1l. In addition, cobalt/nickel ions were doped into CuO nanospheres during the cation exchange process. After the calcination process, CoO/NiO-doped CuO nanospheres were obtained. The average diameter of the as-obtained nanospheres is approximately 6.7 μm. Moreover, as shown in Figure 1g−i, the CuO nanowires did not tend to form the nanospheres structure without addition of Co^{2+} and Ni^{2+}, indicating that the added ions play crucial roles in the formation of the nanosphere morphology. This unique and novel characteristic hierarchical heterostructure with 3D grid and laminated nanospheres offers extensive reactive sites and further promotes charge transfer rate and redox reactions.

The structures and morphologies of the preparative products were all studied by applying transmission electron microscopy (TEM) and high-resolution TEM (HRTEM). Figure 2a presents the TEM image of CuO nanowires, which possess an average diameter of approximately 70 nm and smooth surface. The HRTEM image depicted in Figure 2b reveals well-ordered crystal planes, and the corresponding spacings are measured to be 0.233 nm and 0.25 nm, which should be ascribed to the (111) and (11$\bar{1}$) lattice spacings, respectively. Meanwhile, as displayed in Figure 2c, the selected area electron diffraction (SAED) pattern reveals the clear diffraction rings, indicating the CuO has a good polycrystalline structure.[29] The TEM image of the synthesized CoO/NiO−CuO nanospheres is displayed in Figure 2d. Moreover, the HRTEM image depicted in Figure 2e reveals the ordered crystal planes of CoO/NiO−CuO nanospheres, and the spacings were measured to be 0.21 and 0.17 nm, which should be attributed to the (200) and (220) crystal spacings of NiO and CoO, respectively. The observed SAED diffraction rings demonstrate the well polycrystalline character of the synthesized CoO/NiO−Cu@CuO. Furthermore, the EDX spectrum shown in Figure 2i and its corresponding element mapping images shown in Figure 2h of CoO/NiO−Cu@CuO evidenced the presence of Cu, Ni, O, and Co elements with uniform distribution, which confirmed the successful generation of the laminated CoO/NiO−CuO nanospheres. The EDX spectrum of CoO/NiO−Cu@CuO revealed the Cu/O atomic ratio of 1:1.2 and the atomic contents of Co and Ni of 0.19 and 0.74%, respectively.

Additionally, the valence states of Cu, O, Co, and Ni elements of the synthesized materials were all studied by XPS

DOI: 10.1021/acsami.9b20995
ACS Appl. Mater. Interfaces 2020, 12, 2591−2600

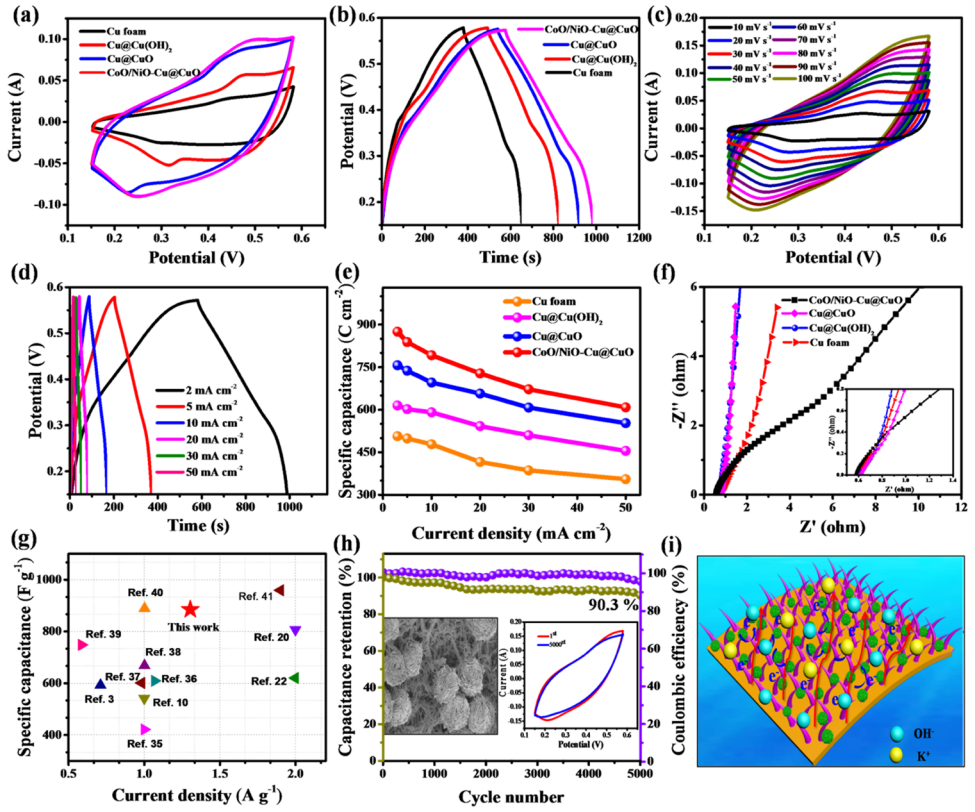

Figure 4. Electrochemical supercapacitance performance tests performed in three-electrode system. (a) CV curves of the fabricated electrodes under a scan rate of 50 mV s^{-1}. (b) GCD curves of the fabricated electrodes under 2 mA cm^{-2}. (c) CV and (d) GCD curves of the CoO/NiO−Cu@CuO electrode tested under different scan rates and current densities. (e) Electrochemical supercapacitance of the prepared electrodes calculated under different current densities. (f) Nyquist plots of the fabricated electrodes. Zoom-in image is shown in the inset. (g) Comparison of the relevant nanomaterials reported in the literature and this work for supercapacitors. (h) Cycle stability and the coulombic efficiency of synthesized CoO/NiO−Cu@CuO electrode during 5000 cycles at 50 mA cm^{-2}; the insets show the SEM image obtained after 5000 cycles and CVs obtained at the 1st and 5000th cycles tested at 100 mV s^{-1}. (i) Diagrammatic sketch for synthesized CoO/NiO−Cu@CuO electrode in enhancing the supercapacitor performance.

analysis. The precursor and stepwise prepared samples were studied using XPS, and the results are shown in Figures S4−S6. The full survey spectrum of the as-obtained CoO/NiO−Cu@CuO material shown in Figure 3a reveals the presence of Cu, O, Co, and Ni elements. Figure 3b displays the Cu 2p spectrum, which can be divided into two major peaks at 932.5 eV (Cu $2p_{3/2}$) and 952.2 eV (Cu $2p_{1/2}$) with three strong statellite peaks located at 940.9, 943.6, and 962.3 eV, which indicated the presence of CuO in the products.[31] The O 1s spectrum displayed in Figure 3c can be divided into three main peaks. It can be seen that two peaks appeared at 531.7 and 529.9 eV, which are attributed to the oxygen atoms. Besides, the peak located at 530.7 eV should be originated from $Cu(OH)_2$. Figure 3e shows the peak of Ni $2p_{3/2}$ located at 855.7 eV and Ni $2p_{1/2}$ appeared at 873.6 eV, which confirms the main composition of Ni^{2+}. Additionally, the peaks appearing at 861.3 and 873.5 eV should be corresponded to the satellite peaks of Ni $2p_{3/2}$ and Ni $2p_{1/2}$, respectively. Co $2p_{3/2}$ located at 780.8 eV can be ascribed to the presence of Co^{2+} ion, which can be observed in Figure 3f.[32] It should be noted that the chemical compositions of the synthesized materials will play critical roles in obtaining the pseudocapacitive electrode with high electrochemical performance. Subsequently, X-ray diffraction (XRD) measurements were then performed to investigate the crystal structure of the synthesized products. As shown in Figure 3d, the as-prepared samples all exhibit strong diffraction peaks located at 43.4, 50.6, and 74.3°, which should be attributed to copper with metallic phase (JCPDS No. 04-0836) originated from the Cu precursor. The observed characteristic peaks of the prepared $Cu(OH)_2$ nanorod arrays should be ascribed to the orthorhombic phase corresponding to JCPDS No. 35-0505, which confirms its successful synthesis. After the calcination process, newly generated diffraction peaks attributed to CuO (JCPDS No. 45-0937) were observed, which clearly indicated the conversion of $Cu(OH)_2$ upon thermal treatment.[30] Additionally, the positions of the CoO/NiO−Cu@CuO peaks corresponded to the standard CoO phase (JCPDS No. 48-1719) and NiO phase (JCPDS No. 44-1159), respectively.

Electrochemical supercapacitor performances of the stepwise fabricated electrodes were all tested through a three-electrode system. The cyclic voltammograms (CVs) of the CoO/NiO−Cu@CuO electrode under diverse scan rate (from 10 to 100 mV s^{-1}) in the voltage range of 0.15−0.58 V are displayed in Figure 4c. As observed, the shapes of CV curves all reveal significant redox peaks characters, indicating that the mechanism mainly depends on the faradaic redox reactions. Meanwhile, with increasing scan rates, the CV curve shape changed slightly except for the increased area. Besides, it can be observed that the current intensity of the fabricated CoO/NiO−Cu@CuO electrode is the highest among all prepared electrodes (Figure S7) when tested at the same scan rates.

DOI: 10.1021/acsami.9b20995
ACS Appl. Mater. Interfaces 2020, 12, 2591−2600

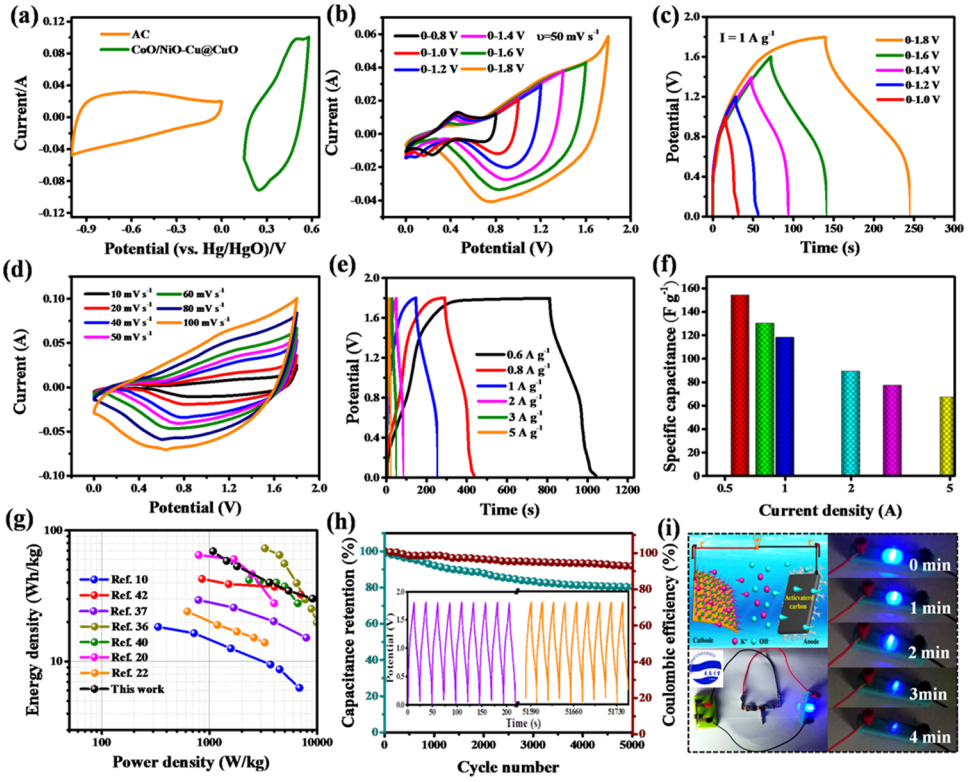

Figure 5. Electrochemical measurements of the fabricated all-solid-state supercapacitor equipment unit. (a) CV curves of AC and CoO/NiO−Cu@CuO electrodes which were separately tested through the three-electrode system. (b) CV and (c) GCD curves measured in diverse voltage windows under the fixed scan rate and current density, respectively. (d) CV curves of the prepared supercapacitor unit measured in the voltage range of 0−1.8 V under diverse scan rates. (e) GCD curves of the fabricated device tested in the voltage window range of 0−1.8 V under diverse current densities. (f) Electrochemical capacitance of the prepared device measured at diverse current densities. (g) Ragone plot of the as-fabricated CoO/NiO−Cu@CuO//AC device compared to the reported literature. (h) Electrochemical cycling stability and coulombic efficiency of fabricated ASC unit tested at 5 A g^{-1} during 5000 cycles; the initial and final several CV cycles are shown in the inset. (i) Schematic configuration of the CoO/NiO−Cu@CuO//AC ASC device and a 2.5 V blue light-emitting-diode indicator powered for 4 min when two as-fabricated ASC devices are in series connection.

Additionally, Figure 4a shows the CVs of all electrodes obtained under the scan rate of 50 mV s^{-1}. As seen, the as-fabricated CoO/NiO−Cu@CuO electrode has the largest CV curve area and strongest redox peak intensity compared to other precursor electrodes, indicating its excellent redox reaction kinetics and outstanding electrochemical properties. The faradaic redox reactions mainly depend on the following valence transition of Cu^{2+}/Cu^{+}, Ni^{2+}/Ni^{3+}, Ni^{3+}/Ni^{4+}, Co^{2+}/Co^{3+}, and Co^{3+}/Co^{4+} reduction couples. Moreover, the electrochemcial supercapacitor performances can be illustrated using the following reactions[33,34]

$$2CuO + H_2O + 2e^- \Leftrightarrow Cu_2O + 2OH^- \; Cu_2O + H_2O + 2OH^- \Leftrightarrow 2Cu(OH)_2 + 2e^-$$

$$CoO + OH^- \Leftrightarrow CoOOH + e^- \; CoOOH + OH^- \Leftrightarrow CoO_2 + H_2O + e^-$$

$$NiO + OH^- \Leftrightarrow NiOOH + e^- \; NiOOH + OH^- \Leftrightarrow NiO_2 + H_2O + e^-$$

In addition, the galvanostatic charge/discharge (GCD) tests of all fabricated electrodes were also carried out, and the curves are displayed in Figure 4b. Moreover, the CoO/NiO−Cu@CuO electrode shows that the discharge time is much longer than that of other precursor electrodes at the same current density of 2 mA cm^{-2}, showing no difference with the CV results. (Figure 4b,d) Furthermore, the discharge time of all electrodes shortens gradually along with the current density increase, agreeing with the CV curve results (Figure S7d−f). In addition, the tested sample electrodes all exhibit similar CV and GCD curve shapes and tendency. The areal supercapacitances of the CoO/NiO−Cu@CuO electrode (Figure 4e) are found to be approximately 875, 838, 792, 727, 672, and 608 C cm^{-2} under diverse current densities from 2 to 50 mA cm^{-2}. As observed, the CoO/NiO−Cu@CuO electrode exhibits the highest supercapacitance among all fabricated electrodes. Additionally, the EIS curves for all fabricated electrodes resulted from the sinusoidal signal are shown in Figure 4f. The internal resistance (R_s) is usually evaluated through the intercept on the x axis, which contains the electrode and electrolyte resistances as well as the interface contact resistance. As shown the inset in Figure 4f, the R_s values of all fabricated precursor electrodes were calculated to be 0.584, 0.597, 0.544, and 0.578 Ω, respectively. In addition, the low R_s implies that the CoO/NiO−Cu@CuO electrode has a good conductivity. Moreover, the semicircle domain in the middle frequency region results from the faradic reactions between Cu^{2+}/Cu^{+}, $Ni^{4+}/Ni^{3+}/Ni^{2+}$, and $Co^{4+}/Co^{3+}/Co^{2+}$ transition. The semicircle diameter means the charge transfer

DOI: 10.1021/acsami.9b20995
ACS Appl. Mater. Interfaces 2020, 12, 2591−2600

resistance (R_{ct}) at interface. As observed, the CoO/NiO−Cu@CuO electrode has a comparatively small semicircle, indicating the lowest R_{ct} among all fabricated electrodes. The Warburg impedance (Z_w) can be valuated through the straight line appearing in the low-frequency region, and the steep slope can explain a low ion-diffusion resistance between the electrode and electrolyte. These above-mentioned results show that the CoO/NiO−Cu@CuO electrode has an excellent electrochemical property. Furthermore, the electrochemical cycle stability of the prepared CoO/NiO−Cu@CuO electrode could be evaluated through the GCD tests. At a high current density of 50 mA cm^{-2}, approximately 90.3% capacitance retention compared to the starting value was observed after 5000 cycles, as shown in Figure 4h. Moreover, the coulombic efficiency based on galvanostatic charge/discharge was measured to be 95.2%. Additionally, the shape of CVs (inset of Figure 4h) obtained at the 5000th cycle is similar to that at the 1st one under the scan rate of 100 mV s^{-1}, indicating the desirable cycling stability of the fabricated CoO/NiO−Cu@CuO electrode. Furthermore, the SEM images of the working electrode of CoO/NiO−Cu@CuO after electrochemical cycling tests further evidence its excellent stability and durability. The morphology of the CoO/NiO−Cu@CuO has no obvious change, as observed from Figures 4h and S9. In addition, under a current density of 0.9 A g^{-1}, the obtained CoO/NiO−Cu@CuO electrode shows an excellent supercapacitance of 885 F g^{-1}, which is comparable to or higher than most of CuO-based electrodes from the literature recently[3,10,20,22,35−41] (Figure 4g). The revealed excellent supercapacitance of the CoO/NiO−Cu@CuO electrode should be caused by the unique morphology of the designed hierarchical heterostructure, as shown in Figure 4i. First, the synthesized laminated CoO/NiO−CuO nanospheres are directly distributed on the 3D grid structure with slightly curly and tops tangled CuO nanowires, which can maintain a fine interfacial contact between the laminated nanospheres and the substrate and provides a more active material for interaction with electrolyte ions. Second, the laminated CoO/NiO−CuO nanospheres on the grid structure reduce the diffusion distance of electrolyte ions and speed up the electron transport rates. This multilevel structure affords more paths for electrolyte shuttling. Thirdly, the laminated nanospheres combined with the 3D grid structure offer a large specific surface area that increases the quantity of reactive sites, resulting in an enhanced electrochemical kinetics. Fourth, the laminated CoO/NiO−CuO nanospheres are generated on the 3D grid structure with strong adhesion as observed in Figure S3, therefore resulting in a prolonged cycling stability of the electrode.

An asymmetric all-solid-state supercapacitor (ASC) equipment unit was prepared by applying the CoO/NiO−Cu@CuO and AC coated with nickel foam as the working and counter electrodes to investigate its practical application of the synthesized material. Figure 5a shows the CV curves of AC and CoO/NiO−Cu@CuO electrodes, which were separately tested through a three-electrode system. The expand voltage range of the device should be caused by both of the fabricated AC and CoO/NiO−Cu@CuO electrodes. The CV and GCD curves tested under diverse voltage range at a fixed scan rate of 50 mV s^{-1} and current density of 1 A g^{-1} are shown in Figure 5b,c. Moreover, the shapes of the CV and GCD curves have no significant change even after the voltage window was expanded to be 1.8 V. The CV curves experimented under diverse scan rates are shown in Figure 5d. The high working potential is beneficial to realize the practical voltage via small devices. Additionally, the GCD curves plotted under various current densities are shown in Figure 5e. The electrochemical supercapacitance is calculated to be approximately 154 F g^{-1} at 0.6 A g^{-1}. Furthermore, the prepared equipment unit achieves an energy density of 69.3 W h kg^{-1} at a power density of 1080 W kg^{-1}, as shown in Figure 5g, which is comparable to or higher than that in the reported literature.[8,10,20,22,36,37,40,42] EIS measurements for the CoO/NiO−Cu@CuO//AC ASC device were performed using a sinusoidal signal with a specific scope (0.01 Hz−100 kHz), which is shown in Figure S8. The equivalent series resistance was calculated to be 1.8 Ω according to the measured Nyquist plots. The slightly decreased conductivity compared to the CoO/NiO−Cu@CuO electrode (0.578 Ω) in a three-electrode system should be ascribed to the binder PVA, which blocks the transport of electrolyte ions. Additionally, the electrochemical supercapacitance can retain approximately 80.1% after 5000 cycles at 5 A g^{-1}, as shown in Figure 5h. Moreover, the coulombic efficiency was measured to be 91.5%. In addition, the schematic diagram of the CoO/NiO−Cu@CuO//AC ASC device prepared using CoO/NiO−Cu@CuO as the working electrode and AC as the counter electrode is shown in the inset of Figure 5i. Furthermore, the commercially applied 2.5 V light-emitting-diode indicator with blue light can be energized for 4 min when two as-fabricated supercapacitor devices are in series connection.

4. CONCLUSIONS

In summary, novel laminated CoO/NiO−CuO nanospheres were successfully generated on $Cu(OH)_2$ nanorod arrays with the assistance of cobalt/nickel ions via facile in situ wet oxidation combined with calcination treatment and cation exchange methods, which was subsequently utilized to prepare a binder-free electrode with an outstanding electrochemical supercapacitance of 875 C cm^{-2} (2035 mF cm^{-2}) at a current density of 2 mA cm^{-2}, remarkable rate capacity of 1395 mF cm^{-2} at 50 mA cm^{-2}, and high cycling stability of 90.3% after 5000 cycles. Furthermore, an all-solid-state asymmetric supercapacitor equipment unit was also fabricated utilizing the CoO/NiO−Cu@CuO hierarchical hybrid and revealed an energy density of 69.3 W h kg^{-1} at a power density of 1080 W kg^{-1}. Moreover, the commercially applied 2.5 V light-emitting-diode indicator with blue light can be energized for 4 min when two as-fabricated supercapacitor devices are in series connection. The outstanding electrochemical performances should be contributed to the novel and unique hierarchical heterostructure of the laminated nanospheres combined with 3D grid structure. Therefore, the prepared hierarchical heterostructure of CoO/NiO−Cu@CuO has enormous potential for the preparation of ultrahigh energy storage devices for practical applications.

■ ASSOCIATED CONTENT

Supporting Information

The Supporting Information is available free of charge at https://pubs.acs.org/doi/10.1021/acsami.9b20995.

Photographs of Cu foam, $Cu@Cu(OH)_2$, Cu@CuO, and CoO/NiO−Cu@CuO; SEM images of Cu foam and CoO/NiO-doped CuO nanospheres; XPS spectra of Cu foam, $Cu@Cu(OH)_2$, and Cu@CuO; CV and GCD

DOI: 10.1021/acsami.9b20995
ACS Appl. Mater. Interfaces 2020, 12, 2591−2600

curves of Cu foam, Cu@Cu(OH)$_2$, and Cu@CuO electrodes; Nyquist plots of the ASC device; SEM images of the CoO/NiO−Cu@CuO electrode after electrochemical tests; specific capacitance with different units of fabricated electrodes; and comparison of relevant nanomaterials for supercapacitors (PDF)

AUTHOR INFORMATION

Corresponding Authors

*E-mail: clzkzy@163.com (L.C.).
*E-mail: jliu@qdu.edu.cn (J.L.).

ORCID

Wenrong Yang: 0000-0001-8815-1951
Jingquan Liu: 0000-0001-6178-8661

Notes

The authors declare no competing financial interest.

ACKNOWLEDGMENTS

This work was supported by National Natural Science Foundation of China (No. 21805124), Shandong Provincial Natural Science Foundation (ZR2018BEM020), and Qingdao Innovation Leading Talent Program.

REFERENCES

(1) Rama Raju, G. S.; Pavitra, E.; Nagaraju, G.; Sekhar, S. C.; Ghoreishian, S. M.; Kwak, C. H.; Yu, J. S.; Huh, Y. S.; Han, Y. K. Rational Design of Forest-Like Nickel Sulfide Hierarchical Architectures with Ultrahigh Areal Capacity as a Binder-Free Cathode Material for Hybrid Supercapacitors. *J. Mater. Chem. A* **2018**, *6*, 13178−13190.

(2) Kandula, S.; Shrestha, K. R.; Kim, N. H.; Lee, J. H. Fabrication of a 3D Hierarchical Sandwich Co_9S_8/α-MnS@N-C@MoS_2 Nanowire Architectures as Advanced Electrode Material for High Performance Hybrid Supercapacitors. *Small* **2018**, *14*, No. 1800291.

(3) Liu, Y.; Cao, X.; Jiang, D.; Jia, D.; Liu, J. Hierarchical CuO Nanorod Arrays: In Situ Generated on Three-Dimensional Copper Foam via Cyclic Voltammetry Oxidation for High-Performance Supercapacitors. *J. Mater. Chem. A* **2018**, *6*, 10474−10483.

(4) Ouyang, Y.; Xia, X.; Ye, H.; Wang, L.; Jiao, X.; Lei, W.; Hao, Q. Three-Dimensional Hierarchical Structure ZnO@C@NiO on Carbon Cloth for Asymmetric Supercapacitor with Enhanced Cycle Stability. *ACS Appl. Mater. Interfaces* **2018**, *10*, 3549−3561.

(5) Zhang, Q.; Zhang, K.; Xu, D.; Yang, G.; Huang, H.; Nie, F.; Liu, C.; Yang, S. CuO Nanostructures: Synthesis, Characterization, Growth mechanisms, Fundamental Properties, and Applications. *Prog. Mater. Sci.* **2014**, *60*, 208−337.

(6) Cao, X.; Wang, X.; Cui, L.; Jiang, D.; Zheng, Y.; Liu, J. Strongly Coupled Nickel Boride/Graphene Hybrid as a Novel Electrode Material for Supercapacitors. *Chem. Eng. J.* **2017**, *327*, 1085−1092.

(7) Wu, C.; Cai, J.; Zhu, Y.; Zhang, K. Nanoforest of Hierarchical Core/Shell CuO@$NiCo_2O_4$ Nanowire Heterostructure Arrays on Nickel Foam for High-Performance Supercapacitors. *RSC Adv.* **2016**, *6*, 63905−63914.

(8) Liu, S.; Ni, D.; Li, H. F.; Jun, S. C.; Hui, K. N.; Ouyang, C. Y. Effect of Cation Substitution on Pseudocapacitive Performance of Spinel Cobaltite MCo_2O_4 (M = Mn, Ni, Cu, and Co). *J. Mater. Chem. A* **2018**, *6*, 10674−10685.

(9) Qu, C.; Liang, Z.; Jiao, Y.; Zhao, B.; Zhu, B.; Dang, D.; Dai, S.; Chen, Y.; Zou, R.; Liu, M. "One-for-All" Strategy in Fast Energy Storage: Production of Pillared MOF Nanorod-Templated Positive/Negative Electrodes for the Application of High-Performance Hybrid Supercapacitor. *Small* **2018**, *14*, No. 1800285.

(10) Guan, H.; Cai, P.; Zhang, X.; Zhang, Y.; Chen, G.; Dong, C. Cu_2O Templating Strategy for the Synthesis of Octahedral Cu_2O@Mn(OH)$_2$ Core-Shell Hierarchical Structures with Superior Performance Supercapacitor. *J. Mater. Chem. A* **2018**, *6*, 13668−13675.

(11) Zhao, Y.; Shi, Z.; Li, H.; Wang, C. Designing Pinecone-Like and Hierarchical Manganese Cobalt Sulfides for Advanced Supercapacitor Electrode. *J. Mater. Chem. A* **2018**, *6*, 12782−12793.

(12) Zhang, Q.; Liu, Z.; Zhao, B.; Cheng, Y.; Zhang, L.; Wu, H.; Wang, M.; Dai, S.; Zhang, K.; Ding, D.; Wu, Y.; Liu, M. Design and Understanding of Dendritic Mixed-Metal Hydroxide Nanosheets@N-doped Carbon Nanotube Array Electrode for High-Performance Asymmetric Supercapacitors. *Energy Storage Mater.* **2019**, *16*, 632−645.

(13) Chen, Q.; Zhao, Y.; Huang, X.; Chen, N.; Qu, L. Three-Dimensional Graphitic Carbon Nitride Functionalized Graphene-Based High-Performance Supercapacitors. *J. Mater. Chem. A* **2015**, *3*, 6761−6766.

(14) Zhang, A.; Li, A.; Zhao, W.; Yan, G.; Liu, B.; Liu, M.; Li, M.; Huo, B.; Liu, J. An Efficient and Self-Guided Chemo-Photothermal Drug Loading System Based on Copolymer and Transferrin Decorated MoS_2 Nanodots for Dually Controlled Drug Release. *Chem. Eng. J.* **2018**, *342*, 120−132.

(15) Zhai, T.; Wang, F.; Yu, M.; Xie, S.; Liang, C.; Li, C.; Xiao, F.; Tang, R.; Wu, Q.; Lu, X.; Tong, Y. 3D MnO_2-Graphene Composites with Large Areal Capacitance for High-Performance Asymmetric Supercapacitors. *Nanoscale* **2013**, *5*, 6790−6796.

(16) Bi, R. R.; Wu, X. L.; Cao, F. F.; Jiang, L. Y.; Guo, Y. G.; Wan, L. J. Highly Dispersed RuO_2 Nanoparticles on Carbon Nanotubes: Facile Synthesis and Enhanced Supercapacitance Performance. *J. Phys. Chem. C* **2010**, *114*, 2448−2451.

(17) Zhang, Y.; Guo, W. W.; Zheng, T. X.; Zhang, Y. X.; Fan, X. Engineering Hierarchical Diatom@CuO@MnO_2 Hybrid for High Performance Supercapacitor. *Appl. Surf. Sci.* **2018**, *427*, 1158−1165.

(18) Bu, I. Y. Y.; Huang, R. Fabrication of CuO-Decorated Reduced Graphene Oxide Nanosheets for Supercapacitor Applications. *Ceram. Int.* **2017**, *43*, 45−50.

(19) Moosavifard, S. E.; El-Kady, M. F.; Rahmanifar, M. S.; Kaner, R. B.; Mousavi, M. F. Designing 3D Highly Ordered Nanoporous CuO Electrodes for High-Performance Asymmetric Supercapacitors. *ACS Appl. Mater. Interfaces* **2015**, *7*, 4851−60.

(20) Kim, H.; Sang, Y. K.; Lun, J. L.; Reddy, A. E.; Gopi, C. V. V. M. Facile One-Step Synthesis of Composite CuO/Co_3O_4 Electrode Material on Ni Foam for Flexible Supercapacitor Applications. *New J. Chem.* **2017**, *41*, 5493−5497.

(21) Zhang, A.; Li, A.; Zhao, W.; Liu, J. Recent Advances in Functional Polymer Decorated Two-Dimensional Transition-Metal Dichalcogenides Nanomaterials for Chemo-Photothermal Therapy. *Chem - Eur. J.* **2018**, *24*, 4215−4227.

(22) Vidhyadharan, B.; Misnon, I. I.; Aziz, R. A.; Padmasree, K. P.; Yusoff, M. M.; Jose, R. Superior Supercapacitive Performance in Electrospun Copper Oxide Nanowire Electrodes. *J. Mater. Chem. A* **2014**, *2*, 6578−6588.

(23) Shinde, S. K.; Fulari, V. J.; Kim, D. Y.; Maile, N. C.; Koli, R. R.; Dhaygude, H. D.; Ghodake, G. S. Chemical Synthesis of Flower-Like Hybrid Cu(OH)$_2$/CuO Electrode: Application of Polyvinyl Alcohol and Triton X-100 to Enhance Supercapacitor Performance. *Colloids Surf., B* **2017**, *156*, 165−174.

(24) Zhao, T.; Yang, W.; Ji, X.; Jin, W.; Hu, J.; Li, T. In-Situ Synthesis of Expanded Graphite Embedded with CuO Nanospheres Coated with Carbon for Supercapacitors. *Appl. Surf. Sci.* **2018**, *460*, 58−64.

(25) Tian, J.; Lin, B.; Sun, Y.; Zhang, X.; Yang, H. Porous WO_3@CuO Composites Derived from Polyoxometalates@Metal Organic Frameworks for Supercapacitor. *Mater. Lett.* **2017**, *206*, 91−94.

(26) Zhou, L.; He, Y.; Jia, C.; Pavlinek, V.; Saha, P.; Cheng, Q. Construction of Hierarchical CuO/Cu_2O@$NiCo_2S_4$ Nanowire Arrays on Copper Foam for High Performance Supercapacitor Electrodes. *Nanomaterials* **2017**, *7*, No. 273.

(27) Jiang, D.; Liang, H.; Liu, Y.; Zheng, Y.; Li, C.; Yang, W.; Barrow, C. J.; Liu, J. In Situ Generation of $CoS_{1.097}$ Nanoparticles on S/N co-Doped Graphene/Carbonized Foam for Mechanically Tough

DOI: 10.1021/acsami.9b20995
ACS Appl. Mater. Interfaces 2020, 12, 2591−2600

and Flexible All Solid-State Supercapacitors. *J. Mater. Chem. A* **2018**, *6*, 11966−11977.
(28) Tamboli, M. S.; Dubal, D. P.; Patil, S. S.; Shaikh, A. F.; Deonikar, V. G.; Kulkarni, M. V.; Maldar, N. N.; Inamuddin; Asiri, A. M.; Gomez-Romero, P.; Kale, B. B.; Patil, D. R. Mimics of Microstructures of Ni Substituted $Mn_{1-X}Ni_XCo_2O_4$ for High Energy Density Asymmetric Capacitors. *Chem. Eng. J.* **2017**, *307*, 300−310.
(29) Liu, J.; Cui, L.; Cao, X.; Sun, X.; Yang, W. A Bunch-like Copper Oxide Nanowire Array as an Efficient, Durable and Economical Catalyst for Methanolysis of Ammonia Borane. *ChemCatChem* **2018**, *10*, 710−715.
(30) Chen, H.; Zhou, M.; Wang, T.; Li, F.; Zhang, Y. X. Construction of Unique Cupric Oxide-Manganese Dioxide Core-Shell Arrays on a Copper Grid for High-Performance Supercapacitors. *J. Mater. Chem. A* **2016**, *4*, 10786−10793.
(31) Ranjith Kumar, D.; Manoj, D.; Santhanalakshmi, J. Optimization of Site Specific Adsorption of Oleylamine Capped CuO Nanoparticles on Mwcnts for Electrochemical Determination of Guanosine. *Sens. Actuators, B* **2013**, *188*, 603−612.
(32) Li, S.; Wang, Y.; Peng, S.; Zhang, L.; Al-Enizi, A. M.; Zhang, H.; Sun, X.; Zheng, G. Co-Ni-Based Nanotubes/Nanosheets as Efficient Water Splitting Electrocatalysts. *Adv. Energy Mater.* **2016**, *6*, No. 1501661.
(33) Zhou, Y.; Zou, X.; Zhao, Z.; Xiang, B.; Zhang, Y. CoO/RGO Composite Prepared by a Facile Direct-Flame Approach for High-Power Supercapacitors. *Ceram. Int.* **2018**, *44*, 16900−16907.
(34) Zhang, X.; Zhang, C.; Abas, A.; Zhang, Y.; Mu, X.; Zhou, J.; Su, Q.; Lan, W.; Xie, E. Ag Nanoparticles Enhanced Vertically-Aligned CuO Nanowire Arrays Grown on Cu Foam for Stable Hybrid Supercapacitors with High Energy Density. *Electrochim. Acta* **2019**, *296*, 535−544.
(35) Zardkhoshoui, A. M.; Davarani, S. S. H. Flexible Asymmetric Supercapacitors Based on CuO@MnO_2-RGO and MoS_2-RGO with Ultrahigh Energy Density. *J. Electroanal. Chem.* **2018**, *827*, 221−229.
(36) Wang, Y.; Wang, S.; Wu, Y.; Zheng, Z.; Hong, K.; Li, B.; Sun, Y. Polyhedron-Core/Double-Shell CuO@C@MnO_2 Decorated Nickel Foam for High Performance All-Solid-State Supercapacitors. *Electrochim. Acta* **2017**, *246*, 1065−1074.
(37) Xu, X.; Liu, Y.; Dong, P.; Ajayan, P. M.; Shen, J.; Ye, M. Mesostructured $CuCo_2S_4$/$CuCo_2O_4$ Nanoflowers as Advanced Electrodes for Asymmetric Supercapacitors. *J. Power Sources* **2018**, *400*, 96−103.
(38) Xu, J.; Wang, Y.; Cao, S.; Zhang, J.; Zhang, G.; Xue, H.; Xu, Q.; Pang, H. Ultrathin Cu-MOF@δ-MnO_2 Nanosheets for Aqueous Electrolyte-Based High-Voltage Electrochemical Capacitors. *J. Mater. Chem. A* **2018**, *6*, 17329−17336.
(39) Gui, Q.; Jiang, J.; Li, Y.; Liu, J. One-Pot Growth of $Co(OH)_2$ Nanowire Bundle Arrays on in Situ Functionalized Carbon Cloth for Robust Flexible Supercapacitor Electrodes. *Dalton Trans.* **2018**, *47*, 15416−15423.
(40) Zhou, S.; Ye, Z.; Hu, S.; Hao, C.; Wang, X.; Huang, C.; Wu, F. Designed Formation of Co_3O_4/$ZnCo_2O_4$/CuO Hollow Polyhedral Nanocages Derived from Zeolitic Imidazolate Framework-67 for High-Performance Supercapacitors. *Nanoscale* **2018**, *10*, 15771−15781.
(41) Meng, F. L.; Zhong, H. X.; Zhang, Q.; Liu, K. H.; Yan, J. M.; Jiang, Q. Integrated Cu_3N Porous Nanowire Array Electrode for High-Performance Supercapacitors. *J. Mater. Chem. A* **2017**, *5*, 18972−18976.
(42) Ensafi, A. A.; Moosavifard, S. E.; Rezaei, B.; Kaverlavani, S. K. Engineering Onion-Like Nanoporous $CuCo_2O_4$ Hollow Spheres Derived from Bimetal-Organic Frameworks for High-Performance Asymmetric Supercapacitors. *J. Mater. Chem. A* **2018**, *6*, 10497−10506.

DOI: 10.1021/acsami.9b20995
ACS Appl. Mater. Interfaces 2020, 12, 2591−2600